AN ACTIVE CONTROL SYSTEM FOR THERMAL FIELDS IN HYPOTHERMIA PROCESSES

C.G. Ambrose ■ Biomedical Engineering Department, The University of Texas at Austin, Austin, TX
L.J. Hayes ■ Biomedical Engineering Program, Aerospace Engineering and Engineering Mechanics Department, The University of Texas at Austin, Austin, TX
G.S. Dulikravich ■ Aerospace Engineering Department, The Pennsylvania State University, University Park, PA

Although cell suspensions, such as blood, are currently preserved through freezing techniques, successful cryopreservation has not been performed on entire organs. This is due in part to the difficulty in maintaining uniform cooling rates throughout a bulk sample. In this work, an optimization procedure was used to determine numerically the proper surface thermal conditions in order to maximize local survival throughout the interior of the entire bulk system. The feasibility of using such a procedure for cryopreservation processes and the limitations of such a procedure are discussed.

INTRODUCTION

The survival of living cells after frozen preservation has been clearly established to be a strong function of the temperature-time history of the specimen. Numerous thermal parameters are required to fully specify a freeze-thaw protocol including the cooling and warming rates, nucleation and storage temperatures, and the intermediate isothermal holding periods. However, research has indicated that the cooling rate is a most crucial factor in determining the ultimate survival of a cell (1). This phenomena is illustrated effectively by a typical cell survival signature where the measured post-thaw survival is expressed as a function of the cooling rate during freezing. Typically, these curves are bell shaped, with a maximum survival at an intermediate cooling rate, above and below which the survival decreases rapidly. An example curve is shown in Figure 7.

When preserving living human bulk tissues (veins, valves, ligaments, embryo, bone, etc..) for the purpose of transplantation, the tissue is cooled in a cryoprotective agent (CPA) to a prescribed low temperature and held at this temperature until used. In practice, optimal survival can only be obtained throughout a specimen when a nearly constant localized cooling rate can be achieved and maintained throughout the specimen. Two factors are primary deterrents to achieving this idealized cooling process. First, since all real systems have finite dimensions, thermal transport properties, and latent heats, the surface thermal conditions are not propagated uniformly into the interior. Second, it is not known *a priori* how the surface conditions should be manipulated to create and maintain optimal local cooling throughout the specimen.

Once the optimal cooling rates for each type of tissue have been determined experimentally, one would like to determine the proper surface thermal conditions so that the optimal local cooling rates are achieved at each instant of time and at every point in the tissue. However, these surface thermal conditions are very difficult to determine because of the irregular shape of human organs and the fact that different cell types have different optimal cooling rates. Experiments have shown that although a whole organ does not survive freezing, cells and parts of the organ do survive. At the present time, freezing protocols tend to use a single cooling rate to determine the surface thermal conditions. In bulk systems, this procedure results in considerable variations of local cooling and survival rates since thermal boundary conditions are not propagated uniformly into the interior of the system (2). Thus, in general no single value of a surface cooling rate can be used to effectively control survival rates in the interior of a bulk container. In fact, the cooling rates may differ by more than an order of magnitude between the surface and deep in the interior of the organ (3) The ability to adjust surface conditions so as to effect desired cooling rates throughout the organ would represent a significant advancement.

The purpose of this work will be to prove the feasibility of using an inverse design or optimization technique (4,5,6) to determine numerically the surface thermal conditions required to maximize local survival throughout the entire organ or bulk sample. This technique will be used to determine surface temperatures that will effect a nearly constant cooling

rate at interior locations in human tissue. Initially, one guesses the surface cooling conditions. Since survival is directly related to cooling rates, one can initially use local optimal cooling rates to describe the container surface thermal conditions and then iteratively adjust the surface temperatures in an attempt to match the local prespecified rates. During each optimization iteration, a two-dimensional unsteady heat conduction equation is solved using the finite element method. This discussion focuses on tissue cooling and does not include latent heat release during phase change. However, this simple case can be used to prove the validity of the basic concept and the applicability of the inverse design procedure. Since any criteria at interior locations can be used in this optimization procedure, this active control concept can be applied to regulate interior temperatures both for cryopreservation, cryosurgery or hyperthermia procedures.

METHODS AND MODEL

A two-dimensional finite element model was used to solve the transient heat conduction equation:

$$-\nabla\cdot(k\nabla T) + \rho c_p \partial T/\partial t = 0 \qquad (1)$$

The timestepping scheme used was a backward finite difference method and quadratic isoparametric elements were used in space. The program produced values of the temperature as a function of time and position, which were then used to calculate local temperature histories and cooling rates. The Davidon-Fletcher-Powell (DFP) conjugate gradient method was chosen (4,5) to determine the search direction in terms of the optimization variables for each iteration. A curve fitting routine was then used to find the minimum error in the specified direction.

The optimization variables were chosen to be the temperatures of the boundary nodes at each successive timestep. Due to the irregular geometries found in many biological systems, it was desired to allow the temperature to vary as a function of position around the boundary. However, allowing each node along the boundary to be specified separately could result in a search region of very large dimensions. Instead, Chebychev polynomials (7) were selected to approximate the circumferential variation of temperatures on the container wall in terms of scaled angular positions of the boundary nodes. The coefficients of these polynomials would then be the optimization variables, (4,5) which could greatly reduce the dimensions of the search region. Seventh order polynomials were chosen to provide a wide spectrum of possible functions around the boundary while limiting the number of variables to seven.

The objective of the optimization was to minimize the difference between the actual cooling rate and the specified optimum rate at every interior node. A weighted root-mean-square error calculation was used to determine the value of the objective function at every timestep:

$$F(X) = \frac{\sum_{i=1}^{\text{nodes}} \left(\sqrt{(CR_i - CR_{opt_i})^2 \cdot w_i} \right)}{\sum_{i=1}^{\text{nodes}} w_i} \qquad (2)$$

Since cells are most sensitive to cooling rates at high subzero temperatures, the cooling rates for the error function were calculated only within a specified temperature range of 0°C to -20°C. The local cooling rate was defined to be a time-averaged value within this temperature range. The time-averaged value has the advantage of canceling small errors at each step, whereas instantaneous rate calculations could introduce small errors at each step that could accumulate to form large errors at the end of the simulation.

At each step in the simulation, the temperature of each node was checked to see if it fell within the specified temperature range. Only the nodes in this range were included in the error calculation. The optimization routines predicted the values of the boundary nodes for the next timestep by varying the boundary conditions, running the finite element code for one timestep, and calculating the resulting error. The optimization routines continued to vary the boundary conditions until an error was found that fell within the tolerance, or until a maximum number of iterations occurred. The initial guess of the boundary temperature for each optimization step was based on the final surface cooling rate value during the previous timesteps.

In any optimization scheme, it is desirable to know both the gradient vector and the hessian matrix in order to determine the best search direction. However, these calculations are often expensive and require large storage spaces. The variable metric methods retain information about previous iterations in an array which approximates the hessian matrix but the hessian is never explicitly determined. This type of method has convergence characteristics similar to second order methods were the hessian is calculated but has fewer computations. In the DFP routines, the search direction at the n^{th} iteration is: (8,9)

$$S^n = -H^n \nabla F(X^n) \qquad (3)$$

Originally, H was taken to be the identity matrix. In subsequent iterations, H was calculated by Equation (4) which approaches the inverse of the hessian as the number of iterations increased.

$$H^{n+1} = H^n + D^n \qquad (4)$$

Where:

$$C^n = (pp^T)/\sigma - [H^n y(H^n y)^T]/\tau \quad (5)$$

$$p = X^n - X^{n-1} \quad (6)$$

$$y = \nabla F(X^n) - \nabla F(X^{n-1}) \quad (7)$$

$$\sigma = p \cdot y \quad (8)$$

$$\tau = y^T H^1 y \quad (9)$$

Once a search direction is determined, an exponential spline fitting routine was used to find the minimum error. The objective function was calculated for ten values of the design variable vector, the points were fit to the spline, and the minimum of the spline was determined. This value was compared to the actual value of the objective function at that point to determine how well the objective function had been mapped. If the fit was not reasonable, the new point was added to the set, and a new spline was fit. This procedure was repeated until a reasonable estimate of the objective function had been obtained. If the minimum found in the one-dimensional search was within the set tolerance of 0.5°C/min, the optimization routines were terminated and a new timestep was begun. Otherwise, a new search direction was determined, and the spline fitting routine was called. This process was continued until an acceptable error was found or until thirty iterations had been performed.

RESULTS AND DISCUSSION

The code was tested on a simple grid using the material properties of isotonic saline. This material was chosen since the thermal diffusivity is the same order of magnitude of many living tissues and cryoprotective agents as is shown in Table 1 (10). The relatively small thermal diffusivity of these materials presents two major problems to the optimization routines. One, there is a finite delay time before any change in boundary conditions is felt at interior nodes. For this paper, the delay time was defined to be the amount of time before the temperature changed by 0.25°C. This delay time is dependent on radial distance from the boundary, the thermal diffusivity, and the boundary cooling rate. To illustrate this, three runs were made without optimization on the grid shown in Figure 1 where the boundary temperature was specified by constant cooling rates of -2.5°C/min, -5°C/min, and -10°C/min. In all three runs, the entire material was assumed to be saline and the initial temperature was 5°C. Figure 2a shows the temperature history of the boundary node (node 13), a node midway between the boundary and the center (node 7), and the center node (node 1) for the boundary cooling rate of -2.5°C/min. These results indicate that the delay time increases with distance from the boundary. In Figure 2b, the temperature history of the center node for all three cooling protocols is plotted, which clearly shows that the delay time decreases as the boundary cooling increases. These delay times create an instability for the optimization routines since strong boundary fluctuations may not be felt at interior locations for many timesteps.

The second difficulty materials with low thermal diffusivities present is that the interior cooling rates do not increase linearly with boundary cooling rates. For the three runs discussed above, the cooling rates as a function of position are shown in Figure 3. These cooling rates are time-averaged values calculated between the temperatures of 0°C and -20°C. The interior cooling rates decrease with each successive doubling of the boundary cooling rate, but the decrease is not linearly proportional to the increase in boundary cooling. In addition, as the boundary cooling rate increases, the gradient of the cooling rate near the surface of the container becomes greater. Since it is desirable to have constant cooling rates within the specimen being frozen, at higher boundary cooling rates the optimization routines will have to constantly adjust the boundary cooling during the freezing protocol.

The ability of the optimization routines to overcome these two difficulties was tested with the optimum cooling rate at all nodes set to be -2.5°C/min. The grid was again specified to be isothermal initially at 5°C and timesteps of 20 seconds were used. The boundary was cooled at -2.5°C/min until the optimization began when the first node reached the temperature of 0°C. The simulation was run for 1520 seconds at which time the center node reached -20.04°C. This run was compared to the run where the boundary cooled at a constant rate of -2.5°C/min and the results are shown in Figures 4-8. Figure 4 shows the boundary temperature throughout the simulation for a constant cooling rate and for the optimized conditions. The slope of the boundary temperature verses time curve appears to change at 360 and 550 seconds into the simulation. The average value of the boundary cooling is -5.5°C/min. Figure 5a shows the difference in the thermal histories for the center node for both the optimized run and the control run. The point at which the two curves differ substantially is approximately 940 seconds into the simulation which corresponds to a 390 second delay from the second boundary slope change at 550 seconds. The results show little effect at this center node from the first boundary slope change at 360 seconds. Figure 5b, however, indicates that the node midway between the boundary and the center does see an effect from the first boundary rate change. This occurs at 570 seconds into the simulation, which points to a delay of 210

seconds. These delay times correlate well with the times shown in Figure 2a.

Figure 6 shows the cooling rates as a function of position for constant boundary cooling rates of -2.5°C/min and -5°C/min , and the optimized cooling rates. The optimized curve shows interior cooling rates similar to those of the -5°C/min case and indeed the average value of the optimized boundary cooling rate is approximately -5. However, the optimized curve has a smaller slope indicating a more uniform distribution of cooling rates throughout the container. This is especially significant near the boundary. Figure 7 show a typical survival rate signature where cell survival is maximized at -2.5°C/min and maximum survival is normalized to 100%. Figure 8 shows survival verses position for a constant boundary cooling at -2.5°C/min and for the optimized boundary cooling. The optimized run represents an increase in survival of about 12.5% over the control run.

It should be noted that even with the optimization routines, all cooling rates on the interior of the container did not reach -2.5°C/min. The routines described here could be improved if a predictor were added to account for the delay times. For example, currently the error is calculated as the effect of a boundary cooling change after only one timestep which occurs before the full effect is felt throughout the system. If instead the error were calculated as the cumulative effect for a number of timesteps, the optimization routines would more accurately predict the optimum boundary cooling protocol and even better results might be obtained.

CONCLUSIONS

An inverse design technique has been tested on a simple geometry and has effectively predicted the boundary conditions needed to produce uniform cooling on the interior of a container. This work shows that it is feasible to use optimization techniques in a finite element code to predict cryopreservation protocols and significant improvements can be achieved in cell survival over constant boundary cooling . This model will be generalized to three dimensions and will include material property change and latent heat release during phase change. In addition, an adaptive technique will be developed to account for the delay times inherent in biological materials.

NOTATION

Roman Letters

C	A symmetric correction matrix used to update the hessian approximation
C_p	Specific heat at a constant pressure (kJ/kg°C)
F(X)	Objective function in terms of design variables
$\nabla F,X)$	Gradient vector : vector of first partial derivitives of the objective function with respect to design variables
H	Hessian matrix : array of second partial derivitives of the objective function with respect to the design variables
k	Thermal conductivity (W/cm°C)
S	Search direction
T	Temperature (°C)
t	Time (s)
CR	Cooling rate (°C/min)
nodes	Total number of nodes for the finite element grid
X	Vector of optimization variables (design variables)
W	Weight for the error calculation

Greek Letters

ρ	Density (kg/cm^3)

Subscripts and Superscripts

i	node number
opt	optimized
n,n+1	optimization iteration number
T	transpose symbol for vectors, matrices

REFERENCES

1. Mazur, P., Science, Vol. 168, pp. 939-949 (1970).

2. Hayes, L.J., and Diller, K.R., Low Temperature Biotechnology, Emerging Applications and Engineering Contributions , McGrath, J.J. and Diller, K. R., eds., pp. 253-271, ASME Press (1988).

3. Hayes, L.J., Diller, K.R., Chang, H.-J., and Lee, H.S., Cryobiology, Vol. 24, pp. 67-81 (1988).

4. Madison, J.V., Dulikravich, G.S., and Hayes, L.J., Proceedings of the International Conference on Inverse Design and Optimization in Engineering Science, (ICIDES-II), G.S. Dulikravich, ed., Pennsylvania State University (1987).

5. Madison, J.V., "Numerical Analysis and Optimization of Objects Subjected to Unsteady Heat Conduction", M.S. Thesis, Penn. State Univ. (1988).

6. Dulikravich, G.S.,and Hayes, L.J., "Control of Surface Temperatures to Optimize Survival in Cryopreservation," ASME-WAM (in press) (1988).

7. Cheney, W. and Kincaid, D., Numerical Mathematics and Computing, Brooks/Cole Publishing, Monterey, California (1985).

8. Vanderplaats, G.N., Numerical Optimization Techniques for Engineering Design, McGraw-Hill, New York (1984).

9. Dennis, G.E., and Schnabel, R.B., Numerical Methods for Unconstrained Optimization and Nonlinear Equations, Prentice Hall, New York (1983).

10. Bowman, M.F., Cravalho, E.G., and Woods, M., Annual Review of Biophysics and Bioengineering, Vol. 4, pp. 43-80 (1975).

Table 1. Material Properties of Biological Tissues. [Taken from (10)].

Material	ρC_p (J/cm^3 K)	k (W/cm K)
Isotonic Saline	4.180	0.0059
Human Skin	2.644	0.0036
Human Kidney	4.128	0.0055
Animal Muscle	2.295	0.0042

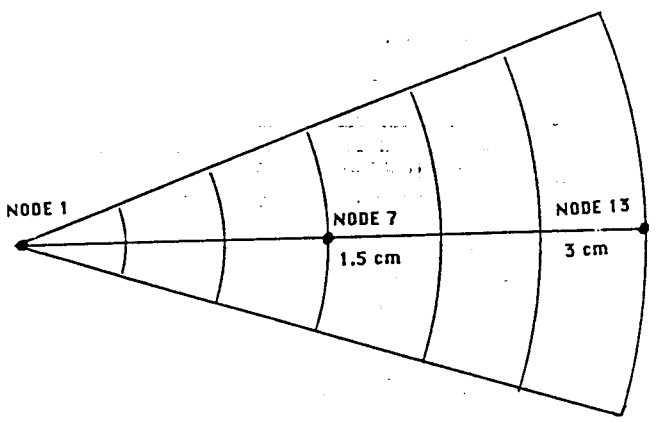

Figure 1. Axisymmetric Finite Element Grid Used to Test the Optimization Code. The Grid Consists of Twelve Quadratic, Isoparametric Elements and has Fifty-nine Nodes.

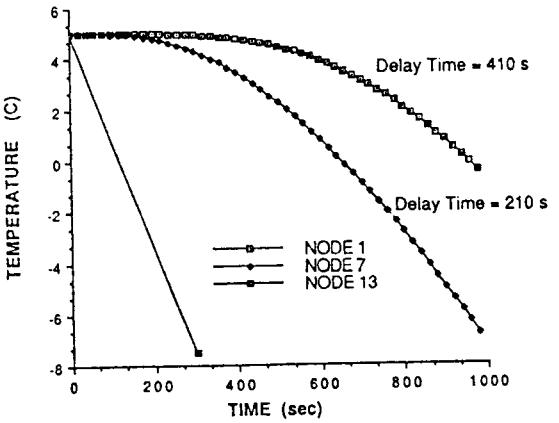

Figure 2a. Thermal Histories for Selected Nodes using a Constant Cooling Rate of -2.5°C/min to Specify Thermal Boundary Conditions.

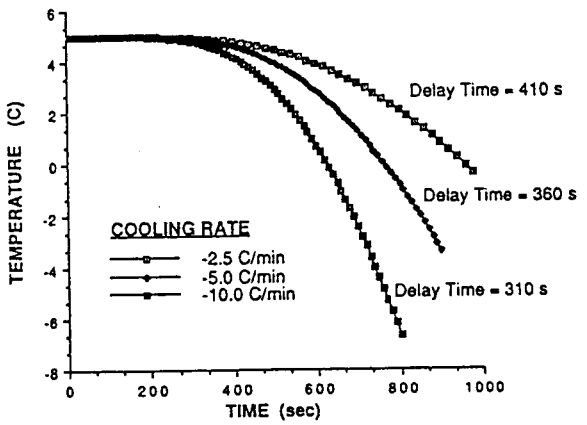

Figure 2b. Thermal Histories for the Center Node for three constant boundary cooling rates of -2.5°C/min, -5.0°C/min, and -10.0°C/min.

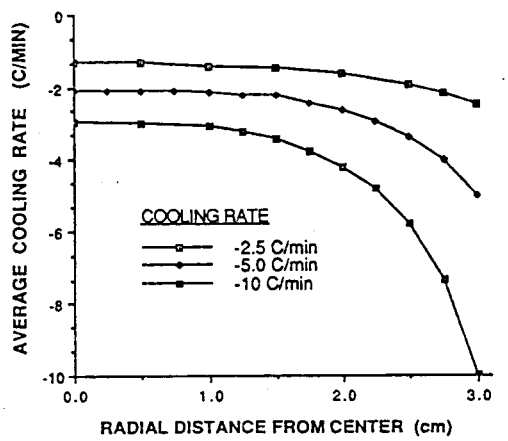

Figure 3. Average Cooling Rates as a Function of Position Within the Container for Unoptimized Cases.

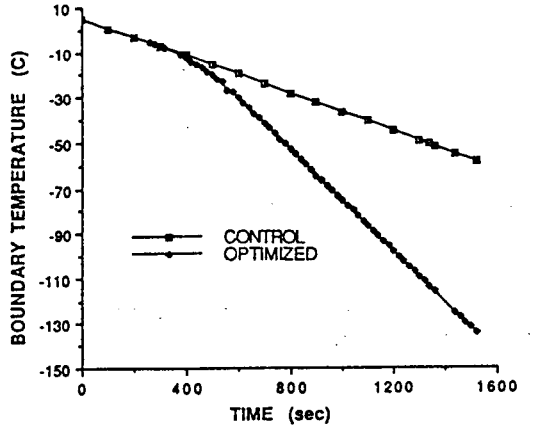

Figure 4. Thermal History for the Boundary for the Control Run of Constant Boundary Cooling at -2.5°C/min, and for the Optimized Case.

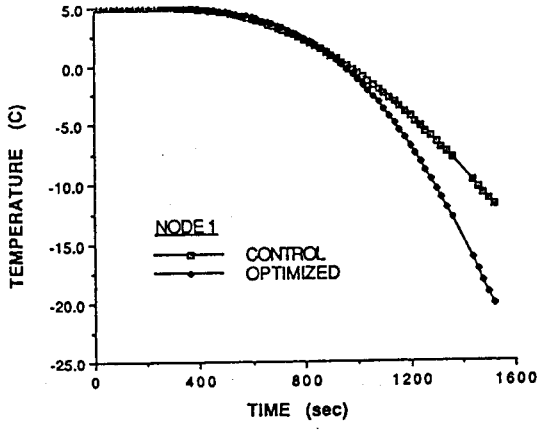

Figure 5a. Thermal History for the Center Node for the Control Run and the Optimized Case.

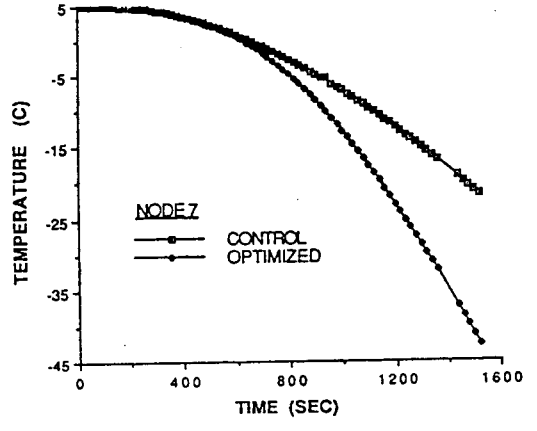

Figure 5b. Thermal History for Node 7 for Both the Control Run and the Optimized Case.

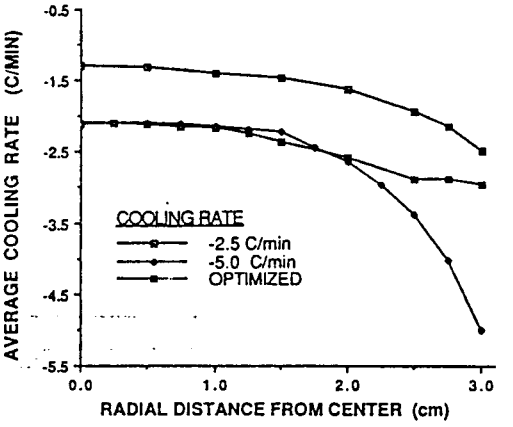

Figure 6. Cooling Rate as a Function of Position for Unoptimized Runs Where the Boundary was Cooled at Constant Rates of -2.5°C/min, and -5.0°C/min, and the Optimized Case.

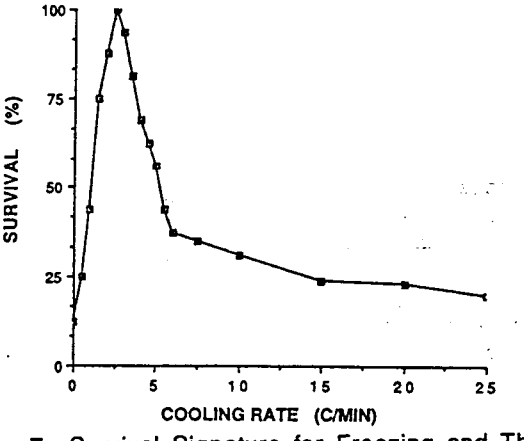

Figure 7. Survival Signature for Freezing and Thawing of Mammalian Cells, as modified from published data (1).

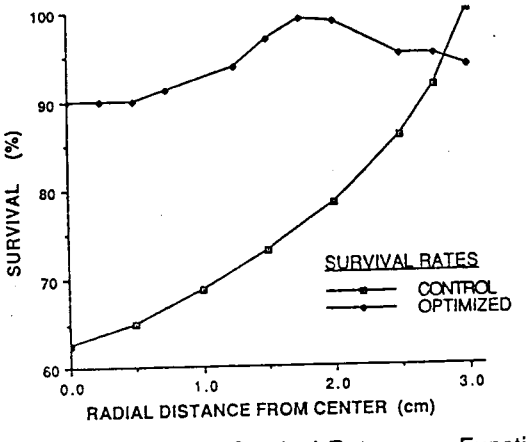

Figure 8. Comparison of Survival Rates as a Function of Position Between the Control Case of Constant Boundary Cooling at -2.5°C/min, and the Optimized Case.